PHYSICAL REVIEW B **84**, 100406(R) (2011)

Finite-temperature phase diagram of the Heisenberg-Kitaev model

Johannes Reuther,[1] Ronny Thomale,[2,3] and Simon Trebst[3]
[1]*Institut für Theorie der Kondensierten Materie, Karlsruhe Institute of Technology, D-76128 Karlsruhe, Germany*
[2]*Department of Physics, Princeton University, Princeton, New Jersey 08544, USA*
[3]*Microsoft Research, Station Q, University of California, Santa Barbara, California 93106, USA*
(Received 16 May 2011; revised manuscript received 29 August 2011; published 23 September 2011)

We discuss the finite-temperature phase diagram of the Heisenberg-Kitaev model on the hexagonal lattice, which has been suggested to describe the spin-orbital exchange in the Mott-insulating iridate Na_2IrO_3. The model exhibits magnetically ordered ground states well beyond the isotropic Heisenberg limit as well as a gapless spin-liquid phase around the anisotropic Kitaev limit. Using a pseudofermion functional renormalization group (RG) approach we extract both the Curie-Weiss scale and the critical ordering scale from the RG flow of the magnetic susceptibility. The Curie-Weiss scale switches sign—indicating a transition of the dominant exchange from antiferromagnetic to ferromagnetic—deep in the magnetically ordered regime for which we find no significant frustration. We discuss our results in light of recent susceptibility measurements for Na_2IrO_3.

DOI: 10.1103/PhysRevB.84.100406 PACS number(s): 75.10.Jm, 71.20.Be, 75.25.Dk, 75.30.Et

In the realm of solid-state physics, frustration refers to the phenomena that arise from the competition between interactions that cannot be simultaneously satisfied: typically a large degeneracy of ground states and a suppression of thermal ordering by fluctuations.[1] For many magnetic solids, *geometric* frustration can arise when interactions are incompatible with the underlying lattice symmetry.[2] A prominent example of the latter are spin-1/2 Heisenberg antiferromagnets on nonbipartite lattice structures, for which there is no straightforward generalization of the Néel state but which can instead harbor more exotic ground states, including commonly elusive spin liquids.[3] Even for bipartite lattices one can encounter geometric frustration when considering orbital degrees of freedom, which occur in a large class of transition-metal oxides that exhibit Jahn-Teller ions.[4] For the latter, crystal-field splitting often results in a single electron (or hole) occupying the doubly degenerate e_g level, for which the orbital occupation is then cast in terms of a pseudospin-1/2. In contrast to ordinary spin degrees of freedom, the exchange interactions between these orbital degrees of freedom—arising from Jahn-Teller distortions and/or superexchange—are highly anisotropic and even for simple bipartite lattices cannot be simultaneously satisfied, which has been shown to result, e.g., in a nontrivial phase diagram of competing orbital orders on the cubic lattice[5] or an orbital Coulomb phase on the diamond lattice.[6]

In this Rapid Communication, we consider a class of materials, certain iridates, where strong spin-orbit coupling (SOC) results in effective degrees of freedom which fall between the two opposing cases above. While iridates have attracted much recent attention as candidate materials for topological insulators,[7] our study is motivated by a family of materials of the form A_2IrO_3, such as Na_2IrO_3, which has recently been shown to be a Mott insulator.[8] In these iridates, the Ir^{4+} ($5d^5$) ions form a quasi-two-dimensional hexagonal lattice of effective $j = 1/2$ momenta. The latter arise from the combined effect of crystal-field splitting of the d orbitals, resulting in a single hole (five electrons) occupying the lowered t_{2g} orbitals, and spin-orbit coupling then giving rise to two Kramers doublets, four electrons filling the (lower) $j = 3/2$ quartet and a single electron in the $j = 1/2$ doublet. The exchange interactions between these effective moments have been argued[9,10] to reflect both the original spin exchange in terms of an isotropic Heisenberg coupling as well as strongly anisotropic orbital interactions in terms of a Kitaev-type exchange

$$H_{\mathrm{HK}}[\alpha] = (1-\alpha)\sum_{\langle i,j\rangle}\vec{\sigma}_i\cdot\vec{\sigma}_j - 2\alpha\sum_{\gamma\ \mathrm{links}}\sigma_i^\gamma\sigma_j^\gamma\,, \qquad (1)$$

where the σ_i denote the effective spin-1/2 moment of the Ir^{4+} ions and $\gamma = x,y,z$ indicates the three different links of the hexagonal lattice. As shown in Eq. (1), all energies are given in units of the Heisenberg coupling divided by $(1-\alpha)$ throughout the article. The two couplings are found[10] to enter with opposite sign, i.e., the isotropic exchange is antiferromagnetic (AFM), while the anisotropic exchange is ferromagnetic (FM). Varying the relative coupling strength $0 \leqslant \alpha \leqslant 1$, the model interpolates from the ordinary Heisenberg model with a Néel ground state for $\alpha = 0$ to the Kitaev model for $\alpha = 1$, which even for FM interactions is highly frustrated and exhibits a gapless spin-liquid ground state.[11] One might thus wonder how the level of frustration varies between the spin- and orbital-dominated limits of this model. This question is also fueled by recent experiments[8] on Na_2IrO_3 that reported magnetic susceptibility measurements, which, besides providing unambiguous evidence of effective spin-1/2 moments, also indicate a considerable suppression for the onset of magnetic correlations below $T_N \approx 15$ K, in comparison with a Curie-Weiss (CW) temperature of $\Theta_{CW} \approx -116$ K. In particular, one might wonder whether this suppression of magnetic ordering might be interpreted as arising from a proximity to the highly exotic spin-liquid phase of the Kitaev model, despite recent resonant x-ray magnetic scattering experiments[12] suggesting a conventionally ordered magnetic ground state.

We address the above questions by investigating the finite-temperature phase diagram of model (1). We use a recently developed pseudofermion functional renormalization group (PF-FRG)[13–15] approach to compute the magnetic susceptibility from the pseudofermion two-particle vertex function evolving under a RG flow with a frequency cutoff Λ. We show that the PF-FRG provides a suitable tool to obtain both finite-temperature and ground-state properties of the model allowing for a direct comparison to thermodynamic experiments.

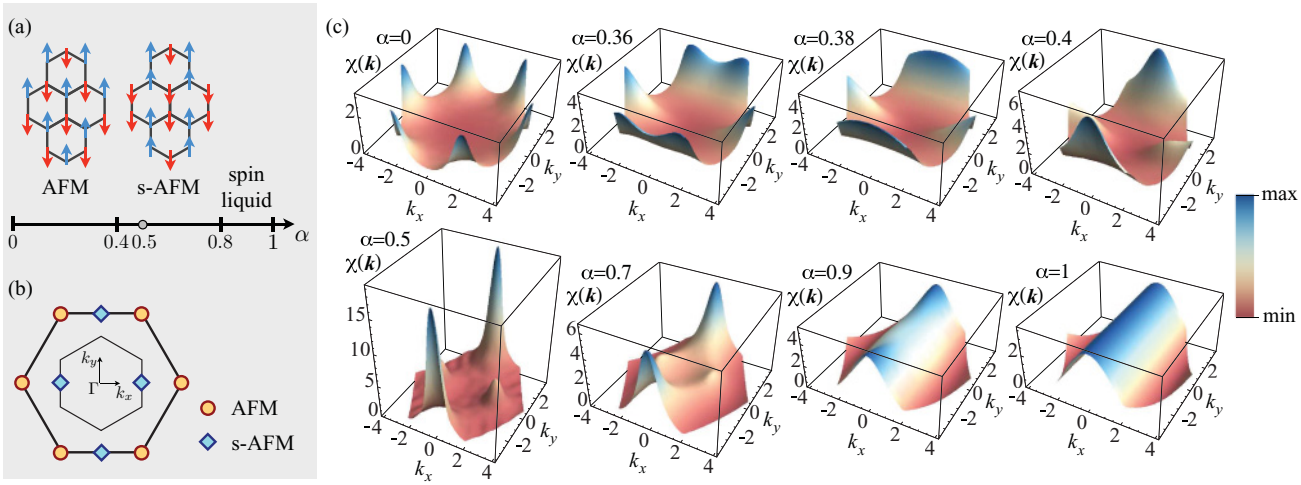

FIG. 1. (Color online) (a) Zero-temperature phase diagram of model (1) exhibiting two magnetic phases (AFM, *s*-AFM) and a spin-liquid phase. (b) Ordering peaks in the extended Brillouin zone (BZ). The inner hexagon indicates the first BZ. *s*-AFM order possesses two inequivalent peak positions in the extended BZ. (c) Evolution of the k-space-resolved static magnetic susceptibility (for a field direction along one of the cubic axes) upon variation of α in (1). The susceptibility has the dimension of an inverse energy.

In particular, we extract the high-temperature CW behavior from the RG flow, the onset of magnetic ordering (from the breakdown of the RG flow), and momentum-resolved magnetic susceptibility profiles, which also allow to identify the nature of the various ground states of model (1).

Numerical simulations. The PF-FRG approach[13–15] reformulates the spin Hamiltonian in terms of a pseudofermion representation of the spin-1/2 operators $S^\mu = 1/2 \sum_{\alpha\beta} f^\dagger_\alpha \sigma^\mu_{\alpha\beta} f_\beta$, $(\alpha,\beta = \uparrow, \downarrow, \mu = x,y,z)$ with fermionic operators $f_\uparrow$ and $f_\downarrow$ and Pauli matrices σ^μ. Such a representation allows to apply Wick's theorem leading to standard Feynman many-body techniques. In this pseudofermion language, quantum spin models become strong-coupling models with zero fermionic bandwidth and a finite interaction strength. The major conceptual advancement of the FRG approach[13,14,16–18] is that it allows to tackle this situation by providing a systematic scheme for the (infinite) self-consistent resummations needed for the strongly coupled fermion problem. The FRG summations are obtained by generating equations for the evolution of all m-particle vertex functions under the flow of a sharp infrared frequency cutoff Λ. To reduce the infinite hierarchy of equations to a closed set, a common approach is to restrict oneself to one-loop diagrams. The PF-FRG extends this approach by also including certain two-loop contributions[19] to retain a sufficient backfeeding of the self-energy corrections to the two-particle vertex evolution. This allows us to compute the magnetic susceptibility—our main diagnostic tool to study model (1).

The FRG equations are simultaneously solved on the imaginary frequency axis and in real space. A numerical solution requires to (i) discretize the frequency dependencies and (ii) to limit the spatial dependence to a finite cluster, thus keeping correlations only up to some maximal length. In our calculations the latter extends over seven lattice spacings corresponding to a cluster size of 112 lattice sites. The onset of spontaneous long-range order is signaled by a breakdown of the smooth RG flow, while the existence of a stable solution indicates the absence of long-range order—see Refs. 13 and 14 for further technical details.

Zero-temperature states. We start our discussion by considering the zero-temperature phases of the Heisenberg-Kitaev model (HKM) (1) and by recapitulating previous $T = 0$ results:[10] The Néel ordered (AFM) state of the Heisenberg limit is stable for $\alpha \lesssim 0.4$, when it gives way to a "stripy" Néel ordered (*s*-AFM) state illustrated in Fig. 1(a) which covers the coupling regime $0.4 \lesssim \alpha \lesssim 0.8$. In the extended parameter regime $0.8 \lesssim \alpha \leqslant 1$ the ground state is a gapless spin liquid (SL) where the emerging gapless excitations are Majorana fermions forming two Dirac cones in momentum space.[11]

We have calculated the characteristic magnetic susceptibility profiles for these states within our PF-FRG approach, as given for various values of α in the main panel of Fig. 1, where we plot the susceptibility just above the (finite) ordering scale Λ_c below which the RG evolution becomes unstable. We adopt the extended Brillouin zone (BZ), illustrated in Fig. 1(b), appropriate for the two-site unit cell of the hexagonal lattice. For the Néel ordered phase we observe characteristic corner peaks in the susceptibility. This magnetic AFM signature remains robust for the full extent of the phase up to $\alpha \approx 0.38$, where we observe a relatively abrupt shift of the susceptibility maxima. The latter is indicative of a first-order phase transition, which is in tune with previous $T = 0$ numerical studies.[10,20] Above $\alpha \approx 0.38$ we observe the onset of the second magnetically ordered phase, the stripy AFM, for which the susceptibility signature comes in the form of *two* (not symmetry-related) maxima, with a dominant peak along $k_x = 0$ in the second BZ and a smaller peak along $k_y = 0$ in the first BZ. From an extrapolation of the finite-temperature crossover line that separates dominant AFM and dominant *s*-AFM fluctuation regimes, we can locate the zero-temperature transition at $\alpha \approx 0.4$, in correspondence with previous studies.[10,20] Within the *s*-AFM phase, the point $\alpha = 0.5$ stands out for which the exact quantum ground state has been shown[10] to be

the classically ordered state (without any dressing). In our calculations, the absence of (quantum) fluctuations at this point is indicated by remarkably sharp response peaks [see Fig. 1(c)]. For $\alpha > 0.5$ we observe a pronounced decrease of the peaks. The phase transition from the *s*-AFM phase to the spin-liquid phase around the Kitaev limit is rather subtle to detect in our calculations. Around the previously reported quantum critical point[10,20] at $\alpha \approx 0.8$ we observe a smooth evolution of the susceptibility profile into the one expected for the SL phase: a pure cos-type susceptibility, reminiscent of the purely nearest-neighbor correlations in this phase.[21]

Finite-temperature physics. To make a connection between the flow parameter Λ and the temperature T, we follow a line of thought discussed by Honerkamp and Salmhofer:[22] Both the flow parameter Λ and the temperature T act as infrared frequency cutoffs. While the former is implemented as a sharp cutoff in the continuous frequency space, the latter allows a description in terms of discrete Matsubara frequencies, where the smallest mesh point sets a lower bound of the energy resolution. Even though the precise cutoff procedures associated with Λ and T are hence quite different, we find that the identification of the two scales leads to qualitatively correct results; quantitative uncertainties possibly enter in our estimates of the ordering instability and its critical scale Λ_c. We note that our numerical simulations are restricted to finite system sizes and thus indicate a *finite* (magnetic) ordering scale even for models with continuous spin symmetry ($\alpha = 0$ and $\alpha = 0.5$), seemingly violating the Mermin-Wagner theorem (MWT) applicable in the thermodynamic limit. However, since the microscopics of any material more often than not relieve the MWT conditions, due to imperfect symmetry or weak three-dimensional (3D) coupling, the estimated Λ_c should provide a good qualitative description of the ordering temperature T_c as observed in experiment.

At high temperatures, we find that the homogeneous susceptibility calculated from the RG flow for various Λ nicely reproduces the expected CW behavior $\chi = C/(\Lambda - \Lambda_{\rm CW})$, as shown in Fig. 2, which allows to extract rather precise numerical estimates for the CW scale $\Lambda_{\rm CW}$ (Fig. 3). Notably, we observe that the CW scale changes sign—indicating a transition of the dominant exchange from AFM to FM—at approximately $\alpha \approx 0.68$, which is still deep in the magnetically ordered regime. Such a change of the dominant exchange is

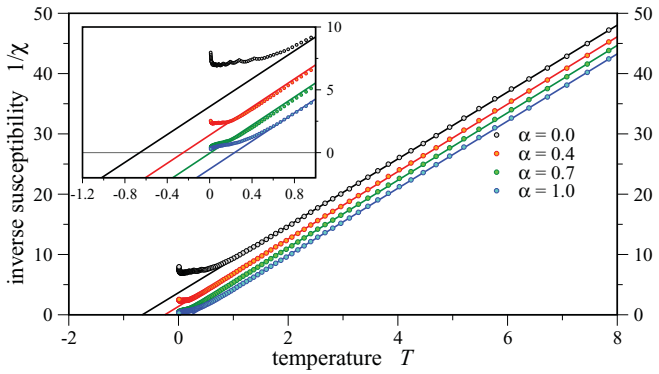

FIG. 2. (Color online) The inverse susceptibility $1/\chi$ as obtained from pseudofermion FRG calculations for various coupling parameters α. The solid lines indicate fits to a CW law.

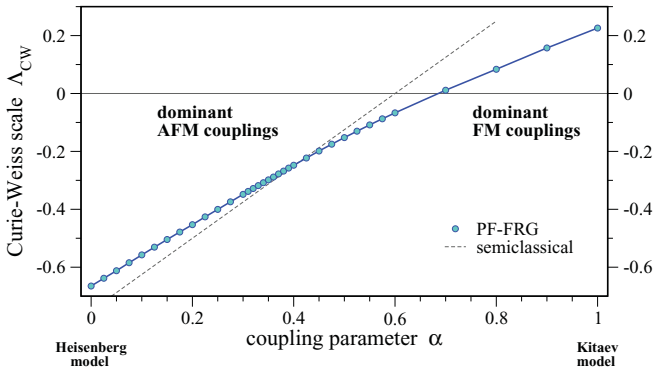

FIG. 3. (Color online) The Curie-Weiss scale $\Lambda_{\rm CW}$ obtained from fitting the inverse susceptibilities in Fig. 2 to a CW law for varying α. At $\alpha \approx 0.67$ the CW scale switches sign, indicating a transition of the dominant exchange from AFM ($\Lambda_{\rm CW} < 0$) to FM ($\Lambda_{\rm CW} > 0$).

already suggestive from a semiclassical analysis of (1), which gives $T_{\rm CW} = -3/4 + 5\alpha/4$ and thus indicates a sign change at approximately $\alpha = 0.6$. This supports that the cutoff Λ indeed retains the features of a temperature parameter and that Λ can be used to deduce finite-temperature properties of model (1).

We can now investigate whether a substantial frustration builds up as one interpolates between the spin-dominated (unfrustrated) Heisenberg regime to the orbital-dominated (strongly frustrated) Kitaev regime. A commonly used measure for frustration is the ratio between CW and ordering scale, the so-called frustration parameter

$$f = |\Theta_{\rm CW}|/T_c \approx |\Lambda_{\rm CW}|/\Lambda_c\,, \qquad (2)$$

with a small value $f \lesssim 5$ indicating the absence of frustration, and systems with $f \gtrsim 10$ being commonly referred to as highly frustrated.[1] We estimate the ordering scale Λ_c from the breakdown of the RG flow, as shown in Fig. 4 for the full parameter range α except for a region around the transition between the *s*-AFM phase and the SL ($\alpha \approx 0.8$), where our approach does not allow to reliably calculate the transition temperature. As shown in Fig. 5, we observe a rather constant

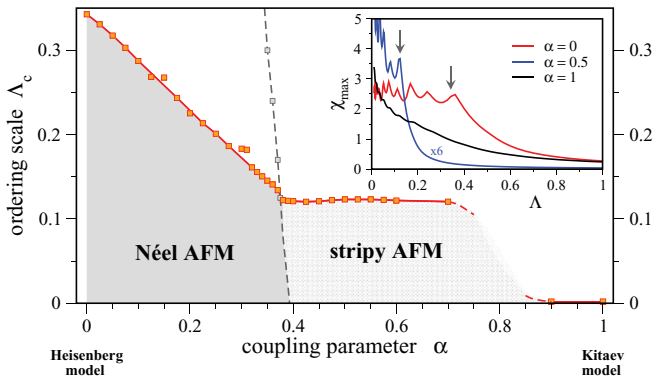

FIG. 4. (Color online) Ordering scale Λ_c obtained from the FRG calculations as a function of α. The dashed line indicates the crossover from dominant AFM to dominant *s*-AFM fluctuations as well as an extrapolation below the ordering transition down to $T = 0$. A regime of enhanced numerical uncertainties is seen near $\alpha \approx 0.8$. The inset shows the RG flow of the magnetic susceptibility versus cutoff Λ. The arrows indicate the Λ_c where the RG flow breaks down.

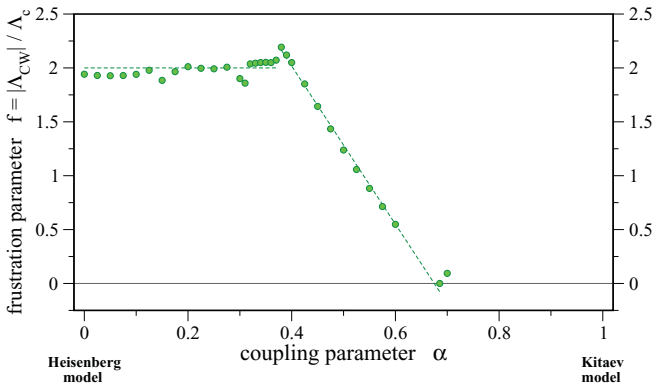

FIG. 5. (Color online) The frustration parameter, i.e., the ratio of Curie-Weiss temperature Λ_{CW} and ordering temperature Λ_c.

plateau $f \approx 2$ for the frustration parameter in the AFM regime before it decreases linearly starting at approximately $\alpha \approx 0.4$ with the onset of the s-AFM phase. At $\alpha = 0.5$ in the s-AFM phase, model (1) can be mapped to a fluctuation-free classical system.[10] This is consistent with our result of $f \approx 1$ at $\alpha = 0.5$, as a frustration parameter close to unity signals the absence of fluctuation-induced frustration. For larger α, the frustration parameter crosses zero as the CW scale changes sign and beyond a regime of numerical uncertainty rapidly diverges as expected for the spin-liquid regime (Fig. 5).

Connection to experiments. We compare our findings to recent thermodynamic measurements[8] on the iridate Na_2IrO_3. The reported CW temperature of $\Theta_{\mathrm{CW}} \approx -116$ K indicates a dominant AFM exchange and the considerable suppression of magnetic ordering down to $T_{\mathrm{N}} \approx 15$ K corresponds to a frustration of $f \approx 8$. While our finite-temperature analysis of the HKM (1) indicates an AFM CW temperature for a wide range of couplings $0 \leqslant \alpha \leqslant 0.68$, the ground states in this regime are relatively simple, magnetically ordered states that do not give rise to a significant suppression of the ordering temperature, as the frustration parameter f never exceeds $f \approx 2$ in our calculations (Fig. 5). On the other hand, we find a strong suppression of the ordering temperature in the spin-liquid phase for $\alpha > 0.8$ and its proximity, but the dominant couplings in this regime are FM ($\Theta_{\mathrm{CW}} > 0$). To reconcile the combination of an AFM CW temperature and a simultaneous suppression of the ordering temperature, one might thus want to look beyond the HKM (1). In particular, one might want to consider various mechanisms that could suppress the ordering temperature in the magnetically ordered regime, such as a next-nearest-neighbor exchange introducing geometric frustration as suggested in Ref. 23 or the role of disorder,[24] especially in the form of nonmagnetic impurities arising from the experimentally observed[8] site mixing between Ir and Na atoms. While the current analysis suggests that Na_2IrO_3 is not in close proximity to the spin-liquid phase of the Kitaev limit, one might still speculate how one could drive the system closer to that regime. One promising path to experimentally increase the anisotropic couplings might be to exert pressure along the ab plane to counteract the c-axis lattice distortion in the material, which quenches the SOC. A similar relief of the lattice distortions might also be expected when replacing the Na ions by smaller Li ions[25] and consider Li_2IrO_3 as a candidate material for more exotic ground states.

R.T. thanks G. Jackeli for a particularly insightful discussions. We further acknowledge discussions with H.-C. Jiang, R. Moessner, and P. Wölfle. R.T. thanks all participants of the "Korrelationstage 2011" in Dresden for discussions. J.R. thanks Microsoft Station Q for hospitality. J.R. is supported by DFG-FOR 960, and R.T. by the Humboldt Foundation.

[1] A. P. Ramirez, Annu. Rev. Mater. Sci. **24**, 453 (1994).
[2] R. Moessner and A. P. Ramirez, Phys. Today **59**(2), 24 (2006).
[3] L. Balents, Nature (London) **464**, 199 (2010).
[4] D. I. Khomskii and M. V. Mostovoy, J. Phys. A **36**, 9197 (2003).
[5] A. van Rynbach, S. Todo, and S. Trebst, Phys. Rev. Lett. **105**, 146402 (2010).
[6] G.-W. Chern and C. Wu, e-print arXiv:1104.1614.
[7] See, e.g., J. E. Moore, Nature (London) **464**, 194 (2010); M. Z. Hasan and C. L. Kane, Rev. Mod. Phys. **82**, 3045 (2010); X.-L. Qi and S.-C. Zhang, e-print arXiv:1008.2026.
[8] Y. Singh and P. Gegenwart, Phys. Rev. B **82**, 064412 (2010).
[9] G. Jackeli and G. Khaliullin, Phys. Rev. Lett. **102**, 017205 (2009).
[10] J. Chaloupka, G. Jackeli, and G. Khaliullin, Phys. Rev. Lett. **105**, 027204 (2010).
[11] A. Kitaev, Ann. Phys. **321**, 2 (2006).
[12] X. Liu, T. Berlijn, W.-G. Yin, W. Ku, A. Tsvelik, Y. J. Kim, H. Gretarsson, Y. Singh, P. Gegenwart, and J. P. Hill, Phys. Rev. B **83**, 220403(R) (2011).
[13] J. Reuther and P. Wölfle, Phys. Rev. B **81**, 144410 (2010).
[14] J. Reuther and R. Thomale, Phys. Rev. B **83**, 024402 (2011).
[15] J. Reuther, D. A. Abanin, and R. Thomale, Phys. Rev. B **84**, 014417 (2011).
[16] C. Wetterich, Phys. Lett. B **301**, 90 (1993).
[17] R. Shankar, Rev. Mod. Phys. **66**, 129 (1994).
[18] C. Honerkamp, M. Salmhofer, N. Furukawa, and T. M. Rice, Phys. Rev. B **63**, 035109 (2001).
[19] A. A. Katanin, Phys. Rev. B **70**, 115109 (2004).
[20] H.-C. Jiang, Z.-C. Gu, X.-L. Qi, and S. Trebst, Phys. Rev. B **83**, 245104 (2011).
[21] G. Baskaran, S. Mandal, and R. Shankar, Phys. Rev. Lett. **98**, 247201 (2007).
[22] C. Honerkamp and M. Salmhofer, Phys. Rev. B **64**, 184516 (2001).
[23] H. Jin, H. Kim, H. Jeong, C. H. Kim, and J. Yu, e-print arXiv:0907.0743.
[24] F. Trousselet, G. Khaliullin, and P. Horsch, Phys. Rev. B **84**, 054409 (2011).
[25] G. Jackeli (private communication).